Materials Chemistry and Physics 263 (2021) 124268

Contents lists available at ScienceDirect

Materials Chemistry and Physics

journal homepage: www.elsevier.com/locate/matchemphys

Electronic structure of defected polyethylene for Schottky emission

Giacomo Buccella [a,*], Davide Ceresoli [b], Andrea Villa [c], Luca Barbieri [c], Roberto Malgesini [c]

[a] Departement of Chemistry, Materials and Chemical Engineering "G. Natta", Politecnico di Milano P.zza L. da Vinci 32-20133, Milan, Italy
[b] Consiglio Nazionale Delle Ricerche, Istituto di Scienze e Tecnologie Chimiche (CNR-SCITEC), I-20133 Milan, Italy
[c] Research Energy System - RSE, Via Rubattino 54, Milan, Italy

HIGHLIGHTS

- Schottky emission (SE) from a neutral polyethylene (PE) surface is unlikely.
- SE is also related to the nature of chemical defects.
- Chemical defects should act as a trap even when the system is charged.
- An oxidized PE surface with an excess electron is consistent with experimental data.

GRAPHICAL ABSTRACT

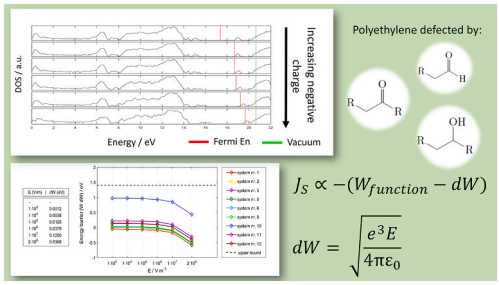

ARTICLE INFO

Keywords:
Electronic structure
Defected polyethylene
Schottky effect
DFT simulations

ABSTRACT

Polyethylene is one of the most used solid state insulators in electrical power industry. It is particularly used to electrically insulate high-voltage cables. Under the stresses associated with AC power supplies, this material undergoes ageing, which is often associated with treeing. It is thought that this phenomenon starts from gaseous defects embedded in the insulator bulk, leading to the formation of a cluster of cavities. Treeing is able to dig the matrix until complete breakdown of the insulating components. Cavities are generated by a sequence of partial discharges. Each discharge is triggered by an electron emission from the surface at the interface with gas. The Schottky effect is believed to be the most likely mechanism able to cause this electron emission.

Our DFT modelling has suggested that electron emission is highly unlikely to occur if the surface is neutral. DOS analysis has revealed that the Schottky effect is also related to chemical defects. The latter must exhibit electronic states slightly under the conduction band. Furthermore, these sites must be able to act as a trap for negative charge excess. A polyethylene system with an excess electron, combined with specific oxidative groups, has proved to be consistent with experimental data.

1. Introduction

The present work is dedicated to the study of the electronic structure of several polyethylene (PE) surface systems, both in pure form and with chemical impurities. For each system, we have performed first-principles calculations in order to obtain the geometry relaxation and the corresponding density of states (DOS). Our aim was to investigate, and describe, the chemical conditions which have to occur to have a

* Corresponding author.
E-mail addresses: giacomo.buccella@polimi.it (G. Buccella), davide.ceresoli@cnr.it (D. Ceresoli), andrea.villa@rse-web.it (A. Villa), luca.barbieri@rse-web.it (L. Barbieri), roberto.malgesini@rse-web.it (R. Malgesini).

https://doi.org/10.1016/j.matchemphys.2021.124268
Received 30 August 2020; Received in revised form 15 December 2020; Accepted 11 January 2021
Available online 28 January 2021

Schottky emission intensity consistent with the recurrence of internal discharges, empirically observed in a number of experiments in polyethylene bulks [1–3]. PE is a widely employed polymer, due to its low cost and suitable dielectric properties. One of its main uses is related to electrical power industry, where it is used as an insulating layer of high voltage cables. It is well known that, under thermal and electrical stresses, this material tends to degrade, usually leading to a complete failure of electrical components [4,5]. This happens in a very unpredictable and irreversible way, causing significant economic damage. In alternated current (AC) power supply systems, the main ageing phenomenon is the treeing [6,7]. The latter consists of a series of electric discharges that cause an accumulation of damages, thus leading to the formation of a cluster of cavities and channels through the polyethylene matrix. These cracks are known as treeing branches. This phenomenon is able to self-sustain, and the branches continue to expand, digging the matrix of the material. Degradation starts in a gaseous defects embedded in the bulk of the insulator, likely formed during the industrial synthesis processes [5], leading to the final breakdown of the insulating layer and the failure of the whole electrical device. In spite of the vast literature on this topic, the evolution of the treeing is still poorly understood and this makes the estimation of the residual life of electrical components very uncertain. The treeing is generated by a sequence of discharges, also known as partial discharges (PDs) which release energy in the material, thus destroying internal chemical bonds. It is believed that each discharge inside the gaseous defect is triggered by an electron emission at the interface, through Schottky effect, see Refs. [8–11]. If the electric field inside the void is strong enough, an electron-avalanche effect will take place [12]. The resulting discharge gives rise to the formation of ions, radicals and other chemical species which make the defect internal atmosphere highly reactive [13–17]. Collisions between these chemicals and the polymeric walls are considered as one of the main causes for treeing propagation [18]. The release of secondary electrons takes place through the Auger effect, and this process contributes to sustain the discharge [19–21]. The Schottky effect is the main discharge inception mechanism considered in a number of simulation tools for PDs such as [3,22,23]. Other effects, such as photoionization and the interaction with cosmic radiation, are considered negligible. They are particularly ineffective in tiny internal voids and channels. Let us consider the experiment performed in Ref. [3] where an isolated void (1 *mm* diameter) in a polymeric bulk has been used. The system has been energized with an industrial AC power supply at 50 *Hz* and nearly one discharge takes place for each period. This means that at least 50 first electrons must be produced for each second. The radiation flux, at sea level, is about 360 $events/m^2$ per second [24]. Just considering the surface of a spherical defect of about 1 *mm* diameter, the number of ionization events would be $\sim 4.5239 \cdot 10^{-3}$ per second which is quite far from the 50 first electrons produced per second in that experiment. The relative interaction probability between the air and the plastic, see Ref. [25], would lead to even lower probabilities. First electron emission can also take place through a tunnelling effect. However, this phenomenon begins to be relevant with electric field values that are beyond the dielectric strength of common industrial insulating materials. Secondary emission is another important mechanism for surface electron ejection. Nevertheless, this mechanism plays a key role in sustaining the discharge rather than causing its inception. Besides, free ions that give rise to secondary emissions are not usually present in the defect atmosphere during inter-discharge periods. As we have outlined, experiments on treeing [6,7,9] and discharges in gaseous defects [3,10,11] have shown that there are conditions under which at least one discharge occurs in each period. And if we assume that each discharge is caused by a Schottky electron, these data, even if indirectly, indicate the existence of a lower bound for the Schottky current. On the other hand, this means that the Schottky work function cannot be higher than a given threshold. In this work we will first estimate this value and then, using some first principle calculations, we will study whether and under what conditions a PE surface may exhibit a similar work function. We have also complemented our analysis by using some parametrized discharge simulations using the techniques described in Refs. [12,26–28]. This allows to estimate also a lower bound for the work function. PE is a very efficient insulator, with an accepted band-gap of 8.8 *eV* in the bulk phase [29]. The experimental work function is 4.9 *eV* [30]. It is well known that bulk PE has a negative electronic affinity (EA), in other words the vacuum level (ε_v) falls below the conduction band minimum. Due to geometric distortions associated with vacuum interface stress, localized shallow states are created at the upper boundary of the valence band (VB) and at the lower boundary of the conduction band (CB). These levels locate ~ 1 *eV* below ε_v [31,32]. In the past, the presence of some chemical impurities capable of significantly modifying the electronic structure of the material, has been linked to the degradation of polymeric insulators under electrical stresses. The electronic structure of PE, with foreign chemical species, presents new additional middle-gap states. That was subject to several computational efforts [33–37]. In the present paper, our aim is to find a defected system capable of giving a Schottky effect with an intensity consistent with the above mentioned discharge experiments. The Schottky current is modelled as a function of the temperature *T*, the applied electric field *E* and the material work function *W*, see Ref. [46]. Nevertheless, it can be verified that the intensity of this current is mainly determined by the value of *W*, which at a microscopic level is determined, in turn, by the electronic structure. For this reason, we obtained, by first-principles calculations exploiting the density functional theory (DFT), the electronic structure and the *W* estimation of various defected PE surface systems. The corresponding relaxed geometries have been considered. Moreover, we have investigated to what extent, the nature of surface chemical defects and charge, affect the probability of Schottky emission. The structure of the paper is the following: In Section 2 we have indirectly estimated an upper bound and lower bound for *W*, referring to an experiment reported in the literature and complementing these data with some simulation analyses. Moreover, we have shown that these values compare well with other estimates used for simulating PDs in internal defects. Section 3 has been devoted to describe how we have estimated *W* from DFT calculation results. In the same section, we have also described the geometric arrangement of the polymer chain that we have chosen to consider throughout this work. Results have been reported and critically discussed in Section 4, and Section 5 provides a final outline.

2. Indirect estimates of Schottky emission

In this section we will show that some discharge experiments, already reported in the literature, may provide some clues to estimate the Schottky current, or at least the corresponding lower and upper bound. Treeing evolution experiments, see Refs. [38,39], may provide some information on the repetition period. However, due to the geometrical and physical complexity associated with this phenomenon, it is difficult to interpret the results. In particular, using an AC power supply, several discharges are usually registered for each period and it is difficult to assess whether one influences the others. Instead, we will consider some more simple configurations, such as the discharges inside isolated voids. This particular setup has been analysed in detail in the literature, both from an experimental viewpoint [40,41] and from that of simulation [42,43]. In this section, we will consider the experimental and numerical results contained in Ref. [3], where the time-sequence of discharges is detailed, and not lumped in the classical phase resolved plot as done, for instance, in Refs. [42,44]. Moreover, the use of an AC energization makes it possible to discard many physical phenomena, such as surface and bulk charge conduction, which dominates the dynamics in DC experiments [40,45].

Let us now briefly review both the setup, depicted in Fig. 1, and the experimental results contained in Ref. [3], where a spherical defect is embedded in the bulk of a polymeric material. The sphere has a diameter of 1 *mm*, and is placed in the middle of a cylindrical sample of

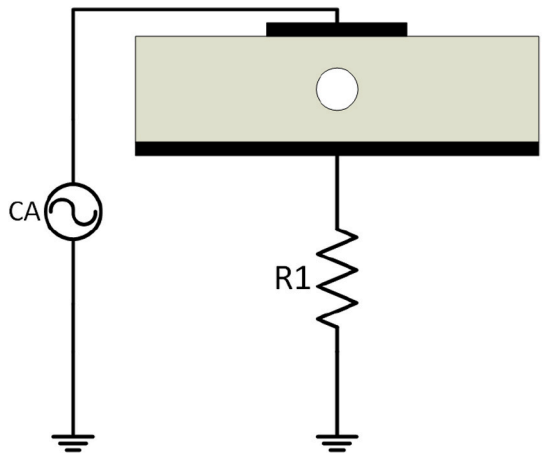

Fig. 1. The experimental setup: a spherical defect is embedded in a cylinder of polyethylene. A couple of electrodes are placed on the faces of the cylinder. The upper plate is connected to a power supply while the lower one is grounded through a resistor.

polyethylene, with a radius of 5 *cm* and a thickness of 2 *mm*. The relative permittivity of PE is assumed to be equal to 2.2. The upper and lower faces of the cylinder are connected to a couple of electrodes, thus the sphere is located 0.5 *mm* from both electrodes. A 50 *Hz* alternated power supply is applied to an electrode, with a peak voltage of 4.41 *kV*, while the other one is grounded. The measurements have shown that, in these conditions, at least one discharge takes place each semi-period.

We have also performed some simulations using the same code developed in Ref. [3] with the aim of determining the influence of the work function on the number of discharge events that take place for each semi-period. We outline that this model takes into account the drift, and diffusion, of charged species coupled with the electrostatic equation. Moreover, the dynamics of neutral species is simulated using the Euler equations of gas dynamics. This provides the pressure and temperature fields in the void. A heat diffusion equation is solved in the bulk and coupled with the heat exchange with the void. This provides an estimate of the temperature both in the void and in the surrounding bulk. Some more details regarding the simulation method can be found in Refs. [26–28] and details of parameters used are included in Table 1.

Table 1
Work functions used for four simulations.

simulation label	*W*/ *eV*	sym time/ *ms*
sym1	0.7	3.4
sym2	1.0	60
sym3	1.3	60
sym4	1.4	60

In Fig. 2 we have shown the evolution of the charge inside the defect. As soon as when a discharge takes place an equal number of electrons and positive ions is created. The mobility of electrons is higher and they collide in a few nanoseconds with the surfaces delimiting the defect, thus creating a positive net charge in the gas. Then ions drift more slowly towards the edges of the sphere recovering the charge neutrality in the void. In other words, each peak corresponds to a discharge event.

Simulation *sym*3 is the same performed in Ref. [3] and, as already shown, we have nearly a discharge for each period in accordance with experimental data. Many other data are produced among which we would like to analyse the temperature field depicted in Fig. 3which plays a major role in Schottky emission. In particular in Fig. 3(a) we have shown the temperature field corresponding to the first discharge which shows that the temperature is almost constant. Moreover in Fig. 3(b) we have shown the temperature field at $t = 52.36$ *ms* where eight discharges have already taken place. As we can see, no major accumulation of thermal energy is observed. The inter-discharge period, nearly 50 *ms*, seems to be largely sufficient to diffuse in the bulk the heat produced by each discharge. This suggests that the Schottky emission is not enhanced by an increase in temperature.

Simulation results can be used to estimate a lower bound for *W*. In fact in *sym*1 we have recorded no discharge. This is due to the fact that the electron current is so strong that it creates a surface charge accumulation such that the internal electric field in the defect almost vanishes. In Fig. 4 we have compared the electric field in *sym*3 (Fig. 4(a)) and in *sym*1 (Fig. 4(b)) at $t = 3.4$ *ms*. In the first case the electric field in the defect is above 5 MV/m and is close to the inception threshold while in the other case the electric field is very weak, well below 1 MV/m.

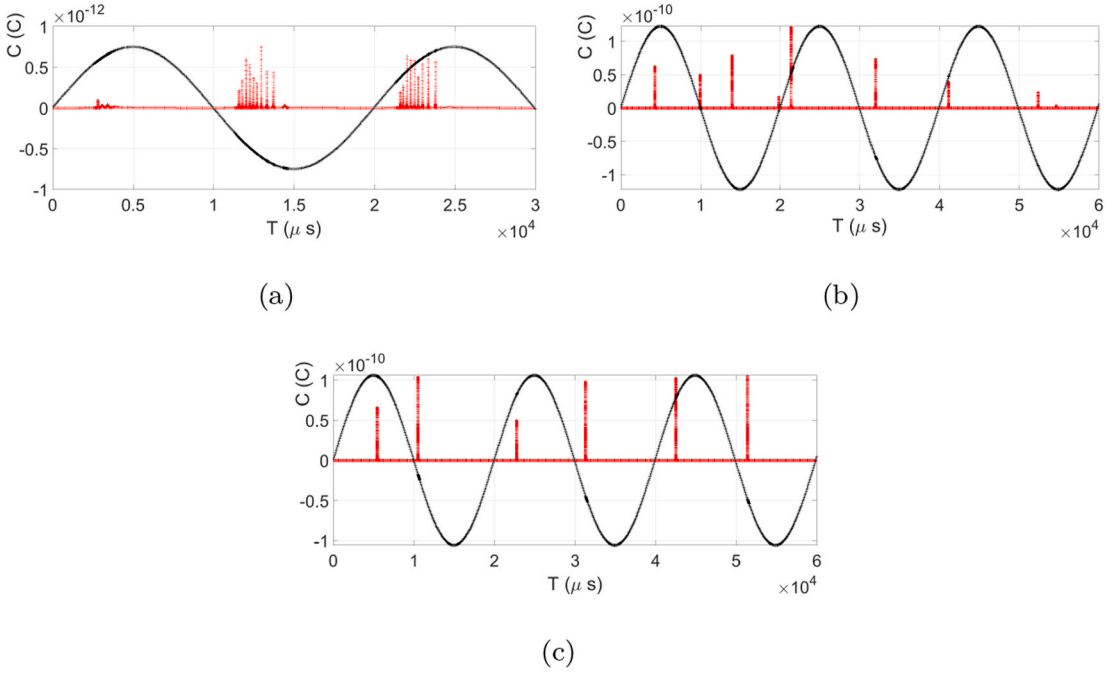

Fig. 2. The evolution of internal charge in the void for simulation *sym*2 (Fig. 2(a)), simulation *sym*3 (Fig. 2(b)) and simulation *sym*4 (Fig. 2(c)).

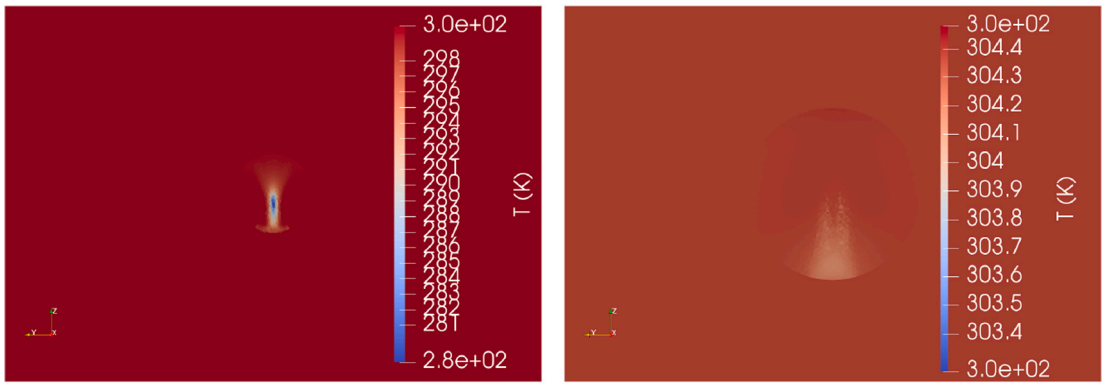

Fig. 3. The temperature field corresponding to the first discharge event (Fig. 3(a)) and to the last discharge event (Fig. 3(b)) in *sym*3.

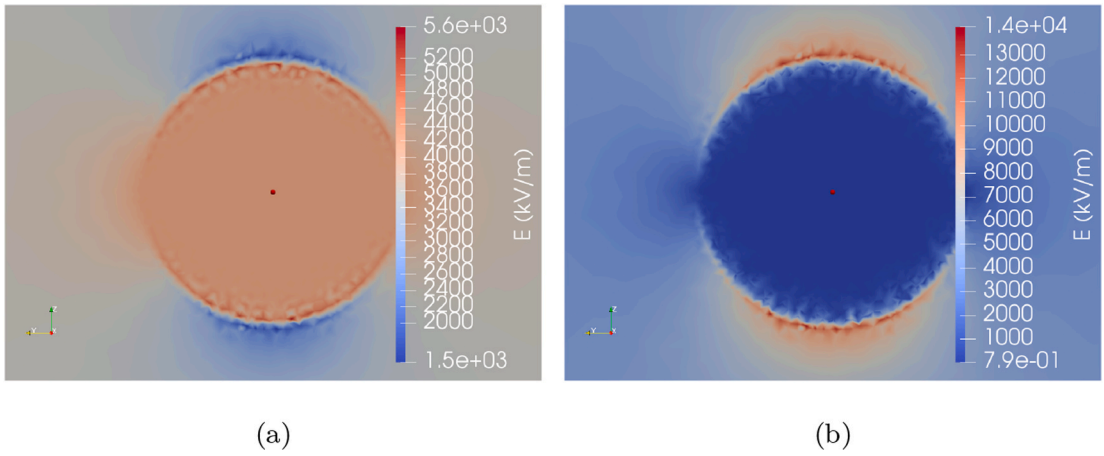

Fig. 4. The electric field in the defect at $t = 3.4ms$ for the *sym*3 simulation (Fig. 4(a)) and for the *sym*1 simulation (Fig. 4(b)).

*sym*2 results are also incompatible with experimental evidences since, as shown in Fig. 2(a), we have got a sequence of tiny multiple discharges for each period. Only simulation *sym*3 (Fig. 2(b)) and simulation *sym*4 (Fig. 2(c)) produce one discharge for each period and, thus, match the experimental results. The values of W associated with these two simulations are quite close to the expected upper bound. In fact, if a discharge takes place each semi-period, it implies that at least one electron is ejected from the surface into the gas in each semi-period, giving rise to the electron avalanche effect. Considering the spherical defect surface $S = 1.2566{\cdot}10^{-5}\ m^2$ it is possible to estimate that the Schottky current density is equal to $J = e/(t{\cdot}S) = 1.2750{\cdot}10^{-12}\ A/m^2$ where $t = 10\ ms$ and $e \simeq 1.6022{\cdot}10^{-19}\ C$ is the electron charge. By substituting the value of J in the equation for the Schottky current

$$J_S = A_g T^2 e^{-\beta(W-dW)}, \tag{1}$$

where

$$dW = \sqrt{\frac{e^3 E}{4\pi\varepsilon_0}}\ , \tag{2}$$

with $\beta = \frac{1}{k_B T}$, we obtain an upper bound for the work function. The pre-exponential factor A_g is typical of the kind of material considered [46], here we take $A_g \simeq 6.0087{\cdot}10^6\ A/m^2K^2$. The temperature T is assumed to be 300 K, $k_B = 8.6167{\cdot}10^{-5}\ eV/K$ is the Boltzmann constant and ε_0 is the vacuum permittivity. Typically, discharges in gases are associated with a local heating and this may alter the surface temperature above the mentioned 300 K, which is the laboratory reference value. It is very difficult to measure the temperature directly inside a tiny void, embedded in a polymeric matrix during a discharge experiment. In this analysis, discharge measurements have been performed just after the energization of the system to preserve the temperature and pressure in void as much as possible. Moreover, the simulation results shown in Fig. 3 suggest that no major heating takes place. Electric field E

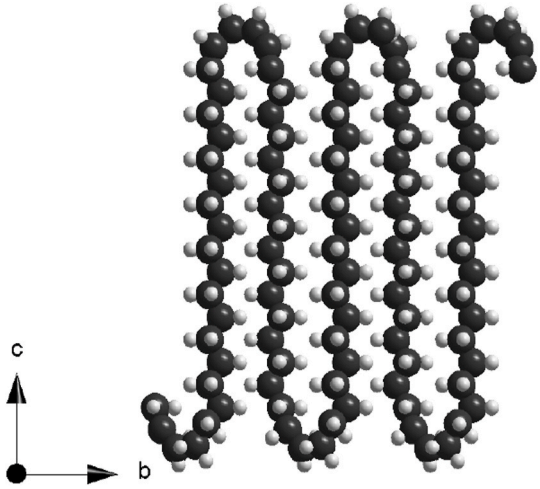

Fig. 5. Polyethylene structure: view along $\vec{a}$ direction.

influences J_S only mildly trough the term dW, defined in Equation (2). Considering a reference maximum electric field intensity $E \simeq 10^2\ MV/m$, which is close to the dielectric strength of some variants of polymers, see Ref. [5], dW reaches a maximum of $\sim 0.5\ eV$. In some more realistic cases, such as the one shown in Fig. 4, where the electric field magnitude is $E \simeq 10\ MV/m$, dW is close to 0.1 eV. Therefore, in this case, W is much larger than dW and dominates the behaviour of J_S.Combining the estimate of J with Equation (1), we can compute the work function upper bound:

$$W - dW = -\frac{1}{\beta} \cdot ln\left(\frac{J}{A_g T^2}\right) \simeq 1.41\ eV \quad . \tag{3}$$

We stress that this estimate is quite similar to the one found in other works related to the measurement and simulation of partial discharges, see Refs. [9–11,47]. In the rest of this paper we estimate, by means of DFT simulations, which conditions must occur to obtain a comparable work function. For the sake of completeness, we also state that multi-stage processes may promote electrons to the vacuum level. In this case an electron in an initial state (i) is first promoted to a middle level (m) and then emitted to the vacuum (v). The probability of transition from state (i) to state (m) is proportional to $e^{-\beta\Delta E}$ where $\Delta E = \varepsilon_{(m)} - \varepsilon_{(i)}$ and $\varepsilon_{(m)}$, $\varepsilon_{(i)}$ are the energies associated with states (i) and (m). Therefore the Schottky current associated with a two step ejection would be

$$J_S = A_g T^2 \cdot \left[e^{-\beta\Delta E} \cdot e^{-\beta(W-dW)}\right] = A_g T^2 e^{-\beta[(W+\Delta E)-dW])}. \tag{4}$$

This suggests that the two step process $(i)\rightarrow(m)\rightarrow(v)$ has the same probability as a single jump $(i)\rightarrow(v)$. However, the specific times scales associated with the relaxation process $(m)\rightarrow(i)$ may make the two step process more unlikely that the one-step process [48].

3. Work function estimation and surface geometry

The work function W is defined as the energy needed to extract an electron from a material, *i.e.*

$$W = \varepsilon_v - \varepsilon_F\ , \tag{5}$$

where ε_F is the Fermi energy, *i.e.* the electron chemical potential at absolute zero, which in some systems could correspond to the occupied level at the highest energy. However, it is known that in PW calculations with pure and neutral insulators, ε_F can be located anywhere in the gap, between the valence band maximum (VBM) and the conduction band minimum (CBM),[1] moreover its location is unpredictable and has no physical meaning [49,50]. Therefore, for systems with no residual charge, Equation (5) results unsuitable to represent the energies at stake, and W has been calculated considering the actual highest energy valence state, *i.e.* the first density peak below ε_F. This latter could correspond to VBM, as happens in pure PE, or to a new state (shallow or deep) created by a foreign chemical species. However, when some electron charge excess is present, the conduction band is forced to populate (as shown in Figs. 7 and 8). In these cases, the Fermi level corresponds, in fact, to the highest electronic energy. Therefore, in charged systems, Equation (5) has been applied. To estimate ε_F, ε_v and the electronic structure of each system, we have used a DFT approach applied to a particular *chain–folded* polymer geometry. This arrangement allows to maintain the continuity of chemical bonds, avoiding any formation of unsaturated centres or exposed methyl groups. This structure is believed to resemble a realistic configuration of the polymer at the interface with an amorphous phase or microscopic vacuum [51,52]. This system has adjacent polymeric chains connected by four methylene units, as shown in Fig. 5. Nevertheless, in the literature, several other arrangements have been considered. For instance, in Ref. [47] authors have performed DFT calculations on the (110) slab of polyethylene.

In [33,34,36,37], authors considered PE with defects such as conjugated double bonds, vinyl groups, hydroxyls and carbonyl groups. However, they performed calculations considering a crystalline or amorphous structure of bulk PE. In this work, we have studied the electronic structure of a vacuum exposed surface, with the arrangement shown in Fig. 5. Moreover, since our aim was to find a system with high ε_F, more forms of oxidation and different radical structures have been included, see Refs. [53,54]. We have considered 20 different surface PE systems, 1 pure and 19 defected, with different combinations (unsaturated centres, oxidations, radicals and others), reported in Tables 2–5.

For *ab − initio* modelling, the Quantum ESPRESSO package has been employed throughout. The latter is an integrated suite of computer codes for solid-state and electronic-structure calculations based on density functional theory, plane waves, and pseudo-potentials [55]. Before obtaining the DOS modelling, the geometry relaxation has been run for each configuration. Starting from the optimized geometry, the plotting of the density of states has been obtained in each case. This has been carried out by firstly performing a self consistent field (*scf*) calculation, which led us to identify the Fermi energy ε_F, key parameter to obtain W from Equation (5). Then, we performed a non-*scf* run at a fixed potential, computed at the previous step, with an increased and uniform sampling of the reciprocal cell. The latter calculation is necessary to obtain the subsequent DOS plotting. In order to facilitate the comparison, each graph has been vertically aligned with the others in correspondence with the first density peak associated with the polymeric chain, by shifting to 0 the first inflection point of the curve (see Figs. 7 and 8). The estimation of the vacuum energy level ε_v has requested the following post-processing. Considering the unit cell of pure and neutral PE, we have extracted the map of the electrostatic potential energy, averaged in the plane perpendicular to the *c*-axis (*i.e.* along the thickness of the slab, see Fig. 5). In the portion of the unit cell corresponding to the vacuum, *i.e.* beyond the surface, the potential energy becomes constant, and ε_v has been estimated as the energy corresponding to this plateau. The same strategy has been widely used in previous studies [21,56–60]. Geometry optimizations and *scf* loops were carried out by setting only one k-point in the Γ position of the Brillouin zone. However, in the non-*scf* runs, the Monkhorst-Pack sampling has been increased with a grid of $12 \times 9 \times 1$ k-points. Ultra-soft pseudo--potentials related to an Hamiltonian with a Perdew-Burke-Ernzerhof exchange-correlation functional, see Ref. [61], were employed throughout. The energy cut-off was set to 35 *Ry* in each calculation. The latter value was considered a valid compromise between accuracy and computational costs after a convergence test we conducted on the optimization of the PE surface cell. The defected structures have been designed, and then optimized, by starting from the neutral pure PE scheme, represented in Fig. 5. The latter was a 25 Å thick slab, with 35 Å of vacuum length.

4. Results and discussion

In this section we present and discuss the results of our calculations. As mentioned above, our calculations aimed at finding a system able to give a Schottky emission current consistent with the discharge period observed in Ref. [3]. The W value has been taken as a benchmark to evaluate the performance of each defected surface. We have listed the W values in Tables 6 and 7, for neutral and charged systems respectively. Below, we have commented the DOS structure of each system, but only those associated with systems *nr*. 1 and 10 have been reported (see Figs. 8 and 7, respectively). For the neutral system *nr*. 10, we also obtained the partial density of states (PDOS), see Fig. 6. For the sake of completeness, although not strictly useful for the present analysis, the graphs of all the other systems have been included in the Supplementary Materials.

[1] In this paper, we refer to VBM and CBM as the energy-gap boundaries of the electronic states associated with the pure polymer, with its distortions due to surface chain-folding.

Table 2
Pure PE and defective systems (no oxidation).

nr.	Name	Structure
1	pe-pure	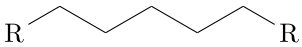
2	pe-db	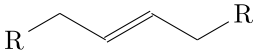
3	pe-cdb	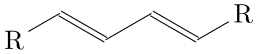
4	pe-vinyl	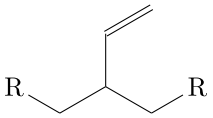
5	pe-amine	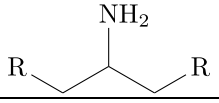

4.1. Neutral systems

We start with treating the defected PE systems listed in Table 2. The double bond (system *nr*. 2) creates a deep state below the Fermi level, detached from VB. A corresponding unoccupied site is created, but slightly overlapped with polymer CB. On the other hand, the conjugated double bond (system *nr*. 3) is capable of forming 2 deep states, one above VB, and one below CB. Our results are in accordance with those in Ref. [36]. The electronic structure features carried by systems *nr*. 3, 4 and 5 are completely comparable with those of system *nr*. 2. Now we pass to consider several types of oxidized systems shown in Tables 3 and 4 The hypothesis on the existence of surface oxidized centres has been suggested by previous experimental measurements, which indicated a noticeable degree of oxidation in untreated industrial PE samples [62–64]. The presence of the carbonyl group, like in system *nr*. 6, is responsible for the appearance of two deep states, one occupied ~ 1 *eV* above VBM, and one unoccupied ~ 1 *eV* below CBM. This outcome is in accordance with those in Refs. [33,36,37]. An analogous situation is obtained with the ring-shaped defect in system *nr*. 8, while an hydroxyl group (system *nr*. 7) creates a single deep state, about ~ 0.8 *eV* above VBM. Combining an aldehyde and an hydroxyl on the surface (system pe-oxidized, *nr*. 9), two pairs of deep states are obtained, with the Fermi energy in the middle. The populated couple is located between 0.8 and 1.5 *eV* above VBM, whereas the unoccupied couple between 0.6 and 1.5 *eV* below CBM. The chemical defects in system *nr*. 10 are designed to reproduce the oxidation degree observed in XPS data [64], which denoted a surface elemental composition ratio O/C = 0.08. Therefore, 3 oxygen atoms (in the form of three detached oxidative groups, see Table 3) have been added to the unit cell containing 40 carbon atoms (41 considering the C in the aldehyde group). As was already the case in system *nr*. 6, the same deep states due to the carbonyl group are formed. Moreover we note that in this case, the corresponding density is approximately double, since there are two C═O groups: an aldehyde (exposed on the surface) and a ketone (about halfway between the two vacuum interfaces). DOS reports another occupied site, slightly overlapped with polymer VB, attributable to the hydroxyl group. Oxidative systems *nr*. 11 and 12 have been examined considering the properties of the corresponding isolated molecules. These are polyphenols, which are natural substances present for example in red fruits, and are known for their antioxidant properties [54]. In fact, their capability to be oxidized

Table 3
Defective systems: oxidations - 1.

nr.	Name	Structure
6	pe-aldehyde	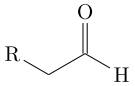
7	pe-hydroxyl	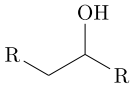
8	pe-1,2-dioxane	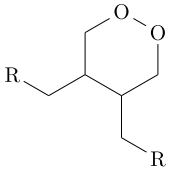
9	pe-oxidized	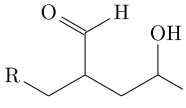
10	pe-Odoped	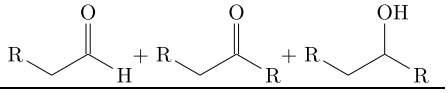

Table 4
Defective systems: oxidations - 2.

nr.	Name	Structure	*nr.*	Name	Structure
11	pe-hydroquinone	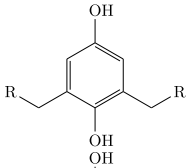	13	pe-diether	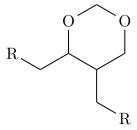
12	pe-catechol	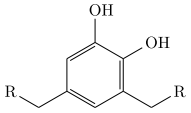	14	pe-diester	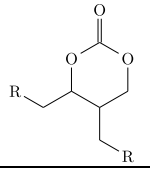

under mild conditions, releasing $2e^- + 2H^+$, is known. However, according to our calculations, this tendency is not reproduced when they are embedded in the polymer chain and surface exposed. These two systems have reported quite similar DOS features, with two states $\sim 1-2$ *eV* above VBM and one ~ 1 *eV* below CBM. As regards system *nr*. 13, DOS presents features similar to those of system *nr*. 7. The diester group in system *nr*. 14 behaves similarly, *i.e*. it does not create an unoccupied state below polymer CB, despite having a carbonyl group.

As we can see by values in Table 6, the *W* of the systems examined so far are too large to get an energy barrier $W - dW$ comparable with our benchmark associated with the Schottky emission. Hence, we decided to test the behaviour of some radical defects, both alone (systems *nr*. 15–17 and 20) and in combination with oxidized systems (*nrs*. 18 and 19). Their presence was not directly suggested by experimental results, however, the energetic stability of these systems has been supported by DFT simulations. The vinyl radical (system *nr*. 15) and the phenyl radical (system *nr*. 17) are, generally, among the most reactive organic radicals [54]. System *nr*. 20 combines an highly reactive radical with an electron donor group, located on the ortho position. Basically, we can infer that the presence of an unpaired electron tends to increase ε_F, which always locates approximately in the middle of the band gap. This site corresponds, in each case, to the energy of the unpaired electron. Nevertheless, the aim of finding a possible defect that lowers the Schottky barrier below the upper bound of 1.41 *eV* is, again, not achieved. None of the defects here presented, both those already considered in simulations of defected PE and those whose existence has just been hypothesised, can match the upper bound described in Section 2 and the estimates proposed in the literature [9–11,47]. To match that magnitude of *W* it is necessary that ε_F increases, up to the conduction states. This could occur if the whole system acquired an excess of electronic charge, in this way the conduction states would be forced to be populated. The next section has been dedicated to the presentation of what has been achieved by imposing different amounts of electronic charge excess to some of the previously considered surface systems.

4.2. Charged systems

In this section we will examine whether, and to what extent, a surface charge may influence *W*. In this paper we do not aim to determine the mechanism which could charge the bulk-gas interface. However, we suggest that many mechanisms could play a role, such as polarization due to the applied electric field. A detailed description of the charging mechanisms is beyond the scope of this paper. Instead, we are interested in describing the conditions under which this excess charge leads to a Schottky emission with an intensity consistent with experiments.

4.2.1. System nr 10

We have performed a series of simulations with increasing charge using the geometrical configuration already depicted in Fig. 5 and considering the 20 types of defects listed in Tables 2–5. Again, to evaluate the compatibility of each system, we refer exclusively to the estimated work function *W*, whose values have been reported in Table 7. We

Table 5
Defective systems: radicals.

nr.	Name	Structure
15	pe-rad-vinyl	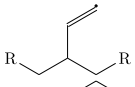
16	pe-rad-branch	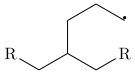
17	pe-rad-phenyl	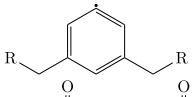
18	pe-rad-Odoped	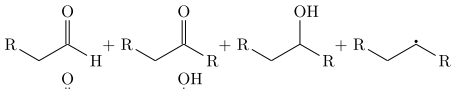
19	pe-rad-oxidized	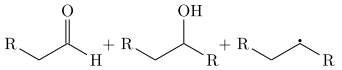
20	pe-rad-phenyl-OH	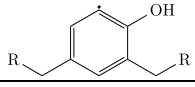

Table 6
Computed W value in eV, neutral systems.

system *nr.*	W/eV	system *nr.*	W/eV
1	4.90	11	4.33
2	5.29	12	4.49
3	4.75	13	4.60
4	4.63	14	5.58
5	4.87	15	4.10
6	4.98	16	3.55
7	5.47	17	3.80
8	4.46	18	2.84
9	4.78	19	3.49
10	4.99	20	4.22

Table 7
Computed W value in eV, charged systems. Charge $= -1$ means that the total charge of the unit cell equals -*e*, *i.e.* one electron charge excess. With charge $= -0.5$ the total charge is $-\frac{1}{2}e$, and so on.

system *nr.*	$W/\ eV$					
charge =	**neutral**	**−0.001**	**−0.01**	**−0.1**	**−0.5**	**−1**
1	4.90	1.04	0.97	0.93	0.07	−0.05
2	5.29					0.00
3	4.75					0.22
5	4.87					0.03
6	4.98					0.15
9	4.78					0.01
10	4.99	1.97	1.96	1.83	1.43	0.97
11	4.33					0.14
12	4.49					0.14

started by considering system *nr*. 10, since its oxidation degree has been designed referring to experimental results [64], as explained in Section 4.1. For this latter system only, we have computed the PDOS of the neutral system, which are shown in Fig. 6. Together with the total DOS of system *nr*. 10, the contributions of p-orbitals associated with all its three oxidizing groups are plotted. From this graph, it can be deduced that the deep state at ~ 19 eV is due to the two carbonyl groups.

When the electronic excess is increased, ε_F grows accordingly. A general charge dependence is observed for the energy position of the deep state. The latter, when the general charge increases, tends to reduce accordingly its detachment from CB, see Fig. 7. With charge $= -1$, this state is observed to partially overlap with the CB, and the work function $W = \varepsilon_v - \varepsilon_F = 0.97\ eV$. The latter value is below the expected upper bound described in Section 2. Compared with the neutral system, both C═O lengths are increased by 0.02 Å. On the other hand, the C–OH bond, remains stable. Therefore, we can state that the topological changes of the chemical bonds due to the charge excess is, in fact, really modest, and that the molecular structure is, in general, not affected. The slight stretching of the C═O lengths indicates that the excess electron

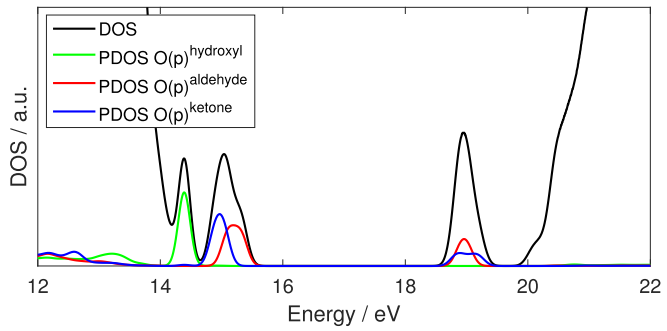

Fig. 6. Neutral pe-Odoped system (system *nr*. 10) DOS and PDOS.

has gone to partially populate both of the carbonyl groups antibonding orbitals π^*. This is in accordance with the results shown in Ref. [37].

4.2.2. The role of chemical defects

In order to see whether this effect could be observed in absence of chemical defects, the same analysis has been carried out for the defect-free PE system (*nr*. 1). The corresponding DOS plots are reported in Fig. 8. If no chemical defects are present, the electronic excess is forced to populate the CB of the insulator. As in the previous case, ε_F increases together with the charge. When $0.5 - 1$ electrons are injected into the CB, it can be seen that ε_F overlaps with the vacuum level ε_v leading to $W \simeq 0\ eV$ (see Table 7). This outcome can be interpreted in this way: in a system free of chemical defects, the electron cannot localize itself. In other words, it does not find any energy hole able to hold it, and thus it remains diffused. This fact contributes to make the ejection a very unlikely event. The observed overlap of the two levels (ε_F and ε_v), denotes that the system has no tendency to host electrons in the CB. It is known that a polyethylene surface, unlike the bulk domain, has slightly positive electronic affinity [32]. However, the hypothetical energy gain due to the electron acquisition, in this case, is not sufficient to compensate the conductive level population of an amount of charge corresponding to one entire elctron. Therefore, this result confirms that the presence of a chemical defect is a key factor to have electron localization, see Refs. [31,37,65]. Moreover, a work function close to 0 is well below the upper bound for W identified in Section 2.

4.2.3. Other impurities response

Since we have provided indications that the presence of chemical defects may play an important role, we further investigate how W is influenced by other types of impurities. For instance, the double bond (system *nr*. 2), in the neutral system, exposes an empty state partially overlapped with CB, but with charge $= -1$, the latter totally overlaps with CB. Also in this case, ε_F is almost superimposed to the vacuum level. Therefore, we can state that the behaviour of system *nr*. 2 is similar to pure PE. On the other hand, the neutral conjugated double bond (system *nr*. 3) has an high energy deep state well detached from CB, similarly to system *nr*. 10. Nevertheless, when the system is charged we observe a behaviour comparable with that of systems *nr*. 1 and 2, although $W = 0.22\ eV$ denotes that the two levels are not exactly overlapped. Anyway, considering the calculation uncertainty, we consider this result comparable to that of systems *nrs*. 1 and 2. When the system includes a different chemical impurity, such as an amine (system *nr*. 5), the behaviour is not dissimilar to that of previous cases, as is summarized in Table 7. The presence of a deep state well detached from CB, seems to be necessary to obtain a non-vanishing W. As it was previously mentioned, the deep state of system *nr*. 10 is due to C═O groups. Carbonyl groups are also present in systems *nr*. 6 and *nr*. 9, therefore we have proceeded to the simulation of these 2 systems with an excess charge. The ring defect in system *nr*. 8 has a different nature but, since it exhibits a deep state similar to that of carbonyl in a neutral case, it is included in the analysis. The electronic structure of charged systems *nr*. 6 and 9 has expressed a behaviour very similar to that of pure PE, *i.e.* ε_F approximately equal to ε_v and $W \sim 0$, see Table 7. This suggests that the carbonyl group of an aldehyde, both alone or coupled with a (likely irrelevant) hydroxyl, is unable to trap the excess electron. This led us to think that the ketone group in system *nr*. 10 could be, in this sense, decisive. During the geometry optimization of the charged system *nr*. 8, the O–O bond tended to stretch until breakage. This effect is likely due to a population increase of an antibonding orbital. However, the verification of this hypothesis is beyond the purpose of the present work. Actually, this is the only case in which the presence of 1 electron excess causes a considerable change in the molecular structure with respect to the corresponding neutral system. In all the other charged systems considered, the structural changes have been very limited compared to the respective neutral systems. According to this DFT prediction, we deduce that system *nr*. 8, if

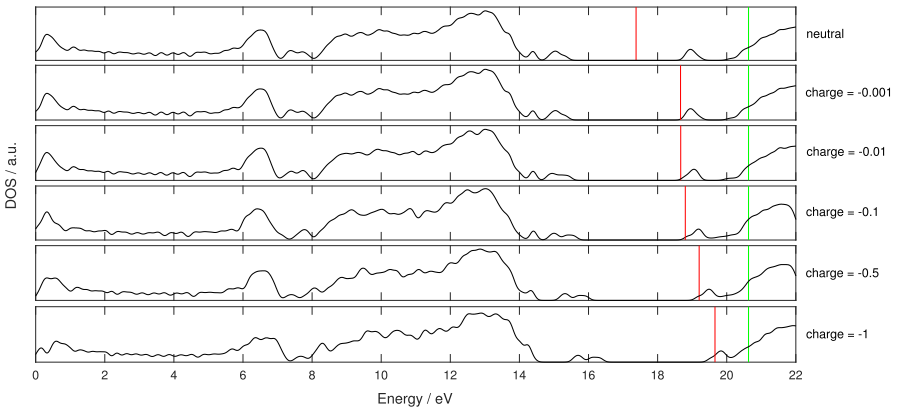

Fig. 7. pe-Odoped system (system *nr*. 10) DOS: increasing charge; ε_F in red, ε_v in green. Charge $= -1$ means that the total charge of the unit cell equals *-e*, *i.e.* one electron charge excess. With charge $= -0.5$ the total charge is $-\frac{1}{2}e$, and so on. (For interpretation of the references to colour in this figure legend, the reader is referred to the Web version of this article.)

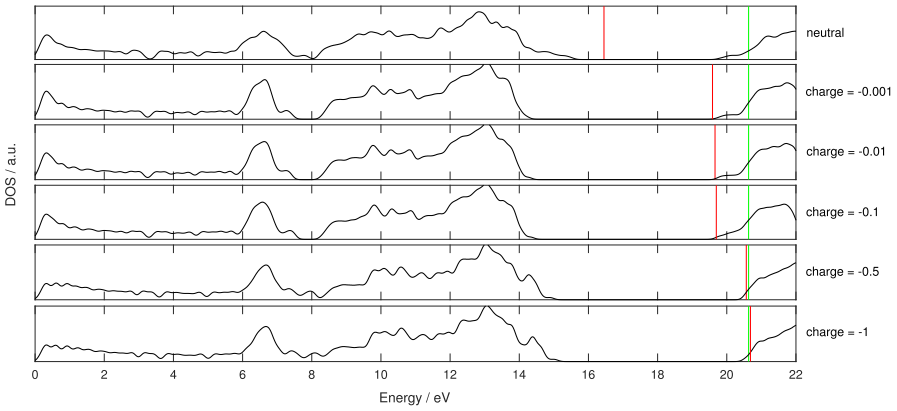

Fig. 8. Pure polyethylene (system *nr*. 1) DOS: increasing charge; ε_F in red ε_v in green. Charge $= -1$ means that the total charge of the unit cell equals *-e*, *i.e.* one electron charge excess. With charge $= -0.5$ the total charge is $-\frac{1}{2}e$, and so on. (For interpretation of the references to colour in this figure legend, the reader is referred to the Web version of this article.)

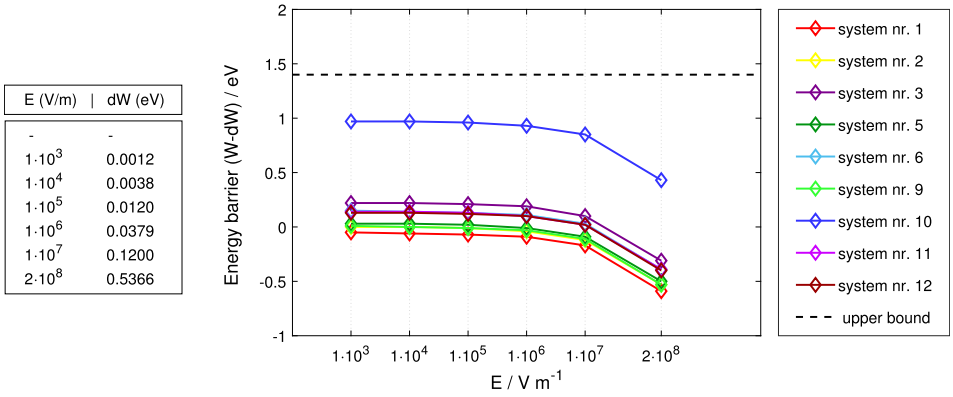

Fig. 9. The decrease of the energy barrier with electric field E in systems with charge $= -1$. Since the contribute dW is a function of the electric field only, the decrease at each step is the same in each plotted series, see table on the left.

charged, is energetically unstable, and that the localization of the excess charge cannot take place without a major modification of the electronic structure, derived from the O–O bond breakage. Therefore, the associated estimate of W, which resulted incompatible with the experimental reference, has been excluded from Table 7. Chemical defects in systems *nr*. 11 and 12 have also been included in the analysis. This has been done to investigate whether, in such circumstances, the aromatic ring could express a sort of electron-hosting property. However, the response of both of them is similar to that of previous cases, see Table 7.

This analysis suggests that the nature of the impurity is also important. In particular, a chemical defect that, in a neutral system, exposes a deep state under CB seems to be necessary, though not sufficient. In fact, and more importantly, it must keep its energy position detached from CB even when it is populated. Among the 20 different arrangements investigated in this work, the system that presented this feature is *nr*. 10 (pe-Odoped). It has three different oxidative groups, well spaced from each other along the PE chain (hydroxyl, aldehyde and ketone, see Table 3). The degree of oxidation is in accordance with experimental surface composition data (XPS) [64]. In the system with charge equal to -1, the high energy orbital that hosts the extra electron belongs to the carbonyl groups (as shown in Fig. 6), and $W = 0.97\ eV$. In the case with charge equal to -0.5, however, the value of $W = 1.43$ is very close to our benchmark. Considering the slight reduction of the barrier due to dW, we can think that in a real system of this type, it is possible to observe Schottky emission even when the average electron excess amount on the surface is lower than 1. The same effect is not observed with an aldehyde group, both when considered alone (system *nr*. 6) and when coupled with an hydroxyl (system *nr*. 9). These data lead us to deduce that the behaviour observed in system *nr*. 10 could be attributable to the ketone group. Moreover, according to our previsions, the contribution dW due to electric field is, in general, negligible for the main part of the E values at stack, as can be seen in Fig. 9.The estimate $W = 0.97$, obtained with system *nr*. 10 and a charge of -1, seems to contradict what we have discussed in Section 2 where the *sym*2 shown in Fig. 2(a) clearly outlines that this value of work function is too small to match the experimental results. DFT itself introduces a certain degree of uncertainty that can explain this discrepancy, however another explanation can be put forward. In fact, DFT results have been obtained using a tiny cell representing a surface element just $Ac = 4.85{\cdot}10^{-10} \times 7.12{\cdot}10^{-10} = 3.4{\cdot}10^{-19}\ m^2$ wide. On the contrary, simulations described in Section 2 use a surface mesh discretization with elements of nearly $10^{-8}\ m^2$. Therefore, large scale simulations must consider a mean W value which is the average of the different values encountered at a microscopic length scale. We may imagine the surface separating the bulk from the void as made of a sequence of cells shown in Fig. 2 among which only a few have a charge. To be more precise, if the ratio between the charged cells and the uncharged ones is equal to $r = e^{-\beta\cdot 1.3}/e^{-\beta\cdot 0.97} \approx 10^{-5}$ then the equivalent macroscopic work function would be exactly 1.3 eV. This hypothesis implies the presence of a surface electron density of $n_e = r/Ac = 2.64{\cdot}10^{13}\ m^{-2}$. Just to compare this datum with other parameters contained in the simulations displayed in Section 2, the electron surface density n_e would generate a normal electric field jump on the surface of $(n_e \cdot e)/\varepsilon_0 = 0.47MV$ which can be compared with the jump displayed in Fig. 4(a). Since, in that case, no discharge has taken place yet, the normal electric field discontinuity is only due to polarization effects: as we can see the magnitude of the jump is about $4MV/m$ and thus it is much greater than $(n_e \cdot e)/\varepsilon_0$. This means that the supposed presence of a surface charge, needed to create a sufficiently strong Schottky emission, does not create an unfeasible electric field, greater that the expected one.

5. Conclusions

In this paper we have detailed in which conditions the Schottky emission from a surface-bulk interface can provide a series of free electrons that cause the inception of a sequence of discharges. In the literature [3,22,23], Schottky emission is considered the most important mechanism for the triggering of the discharges in isolated voids. We have analysed an experimental test case, *i.e.* the one described in Ref. [3], and we have provided an upper and lower bound for the work function, which is the key parameter determining the Schottky emission. This case is representative of many other experiments [40–42] where, however, the details of the discharge sequence are not available. W estimates are consistent with other values used in the literature [9–11,47] that deal with macroscopic plasma-polymer interactions. Therefore, we have tackled this particular problem from a microscopic point of view: some first-principles calculations have been carried out to model the electronic structure and estimate W of 20 different PE surface systems, considering several possible chemical defects. The aim was to find, and describe, a PE system with a W consistent with our experimental reference, *i.e.* under the estimated upper bound. Since a pure and/or neutral PE surface does not provide a valid candidate, we have considered a number of chemical surface defects and an increasing amount of surface charge. Our results seem to point out that both surface charge and chemical defects must be present to justify the emission strength observed in experimental tests described above. However, not all defects are compatible. Among the various chemical impurities considered here, the system containing 3 detached oxidative groups resulted in a W consistent with our predictions. Moreover, we found that the ketone group seems to be decisive for obtaining that value. The oxidation degree of this latter system resembles the XPS data reported in Ref. [64]. While oxidation is quite common, even in not-aged PE surfaces, charge accumulation can be regarded as an open problem. It is still not clear which physical phenomenon may be the main driver for this process, and it would be worth conducting further studies on this. Our estimations are dependent upon the hypothesis that the defected surface is at room temperature. This assumption is backed by both the experimental procedure adopted in Ref. [3] and by a series of simulations performed both in that work and in this one. So far, there is no evidence that the temperature, at least in the experimental case considered in Section 2, is largely different from 300 K. However, we also point out that the estimation of surface temperature in tiny internal defects is challenging both from a computational and experimental point of view, and it would be worth to investigate this aspect further. Other possible emission mechanisms which promote electrons from the bulk to the gas defect may be considered. However, to the best of the authors' knowledge, no other mechanism has been put forward so far. To conclude, we have also shown that the presence of an electric field does not provide a strong contribution dW to the Schottky potential barrier, at least for electric field magnitudes below the dielectric strength of PE.

Declaration of competing interest

The authors declare that they have no known competing financial interests or personal relationships that could have appeared to influence the work reported in this paper.

Acknowledgment

This work has been financed by the Research Found for the Italian Electrical System under the Contract Agreement between RSE and the Ministry of Economic Development. The authors wish to thank L. Barbareschi, A. Buccella, R. Martinazzo, M. Trioni and A. Rognoni for their valuable contributions and suggestions.

Appendix A. Supplementary data

Supplementary data to this article can be found online at https://doi.org/10.1016/j.matchemphys.2021.124268.

References

[1] Proceedings of the 6th International Conference on Properties, Applications of Dielectric Materials, A Comparison between Void and Electrical Treeing Discharges in Polyethylene, Xi'an Jiaotong University, Xl'an, China, 2000.

[2] L. Testa, S. Serra, G.C. Montanari, Advanced modeling of electron avalanche process in polymeric dielectric voids: simulations and experimental validation, J. Appl. Phys. 108 (3) (2010), 034110, https://doi.org/10.1063/1.3359713.

[3] A. Villa, L. Barbieri, M. Gondola, A.R. Leon-Garzon, R. sMalgesini, A PDE-based partial discharge simulator, J. Comput. Phys. 345 (2017) 687–705.

[4] G. Mazzanti, G.C. Montanari, L.A. Dissado, A space-charge life model for a.c electrical aging of polymers, IEEE Trans. Dielectr. Electr. Insul. 6 (6) (1999) 864–875.

[5] S. Serra, G.C. Montanari, G. Mazzanti, Theory of inception mechanism and growth of defect-induced damage in polyethylene cable insulation, J. Appl. Phys. 98 (3) (2005), 034102, https://doi.org/10.1063/1.1978986.

[6] S. Rowland, R. Schurch, M. Pattouras, Q. Li, Application of FEA to image-based models of electrical trees with uniform conductivity, IEEE Trans. Dielectr. Electr. Insul. 22 (3) (2015) 1537–1546.

[7] T. Farr, R. Vogelsang, K. Frohlich, A new deterministic model for tree growth in polymers with barriers. Electrical Insulation and Dielectric Phenomena, 2001 Annual Report, Conference on, 2001.

[8] A. Villa, A.R. Leon-Garzon, L. Barbieri, R. Malgesini, Ignition of discharges in macroscopic isolated voids and first electron availability, J. Appl. Phys. 125 (2019), 043302.

[9] L. Niemeyer, A generalized approach to partial discharge modeling, IEEE Trans. Dielectr. Electr. Insul. 2 (4) (1995) 510–528.

[10] R. Schifani, R. Candela, P. Romano, On PD mechanisms at high temperature in voids included in an epoxy resin, IEEE Trans. Dielectr. Electr. Insul. 8 (4) (2001) 589–597.

[11] A. Cavallini, G.C. Montanari, Effect of supply and voltage frequency and on testing and of insulation and system, IEEE Trans. Dielectr. Electr. Insul. 13 (1) (2006) 111–121.

[12] A. Villa, L. Barbieri, M. Gondola, A.R. Leon-Garzon, R. Malgesini, Stability of the discretization of the electron avalanche phenomenon, J. Comput. Phys. 296 (2015) 369–381, https://doi.org/10.1016/j.jcp.2015.05.013.

[13] S. J. Dodd, A deterministic model for the growth of non-conducting electrical tree structures, J. Phys. Appl. Phys. 36 (129).

[14] H.Z. Ding, B.R. Varlow, Thermodynamic model and for electrical and tree propagation and kinetics in combined and electrical and mechanical and stresses, IEEE Trans. Dielectr. Electr. Insul. 12 (1) (2005) 81–89.

[15] G. Mazzanti, G. C. Montanari, F. Civenni, Model of inception and growth of damage from microvoids in polyethylene-based materials for hvdc cables part 1: theoretical approach, IEEE Trans. Dielectr. Electr. Insul. 14 (5).

[16] G.C. Montanari, Notes on theoretical and practical and aspects of polymeric and insulation aging and key words: aging and life model and electrical stress and reliability and space charge and partial discharge and electrical and insulation, IEEE Electr. Insul. Mag. 29 (2013) 34–44.

[17] A.R. Leon-Garzon, G. Dotelli, A. Villa, L. Barbieri, M. Gondola, C. Cavallotti, Thermodynamic analysis of the degradation of polyethylene subjected to internal partial discharges, Chem. Eng. Sci. 180 (2018) 1–10, https://doi.org/10.1016/j.ces.2018.01.023.

[18] A.S. Vaughan, I.L. Hosier, S.J. Dodd, S.J. Sutton, On the structure and chemistry of electrical trees in polyethylene, J. Phys. Appl. Phys. 39 (5) (2006) 962.

[19] T.N. Tran, I.O. Golosnoy, P.L.L.G.E. Georghiou, Numerical modelling of negative discharges in air with experimental validation, J. Phys. Appl. Phys. 44 (1) (2011), 015203.

[20] L. Binxian, S. Hongyu, W. Qiukun, Characteristics of Trichel pulse parameters in negative corona discharge, IEEE Trans. Plasma Sci. 45 (8) (2017) 2191–2201.

[21] G. Buccella, D. Ceresoli, A. Villa, L. Barbieri, R. Malgesini, First principles evaluation of the secondary electron yield from polyethylene surface, J. Phys. D Appl. Phys. 53 (2020) 175301.

[22] G. Callender, I. Golosnoy, P.L. Lewin, P. Rapisarda, Critical analysis of partial discharge dynamics in air filled spherical voids, J. Phys. Appl. Phys. 51 (2018) 125601.

[23] G. Callender, T. Tanmaneeprasert, P.L. Lewin, Simulating partial discharge activity in a cylindrical void using a model of plasma dynamics, J. Phys. Appl. Phys. 52 (2019), 055206.

[24] J.F. Ziegler, Terrestrial cosmic rays, IBM J. Res. Dev. 40 (1) (1996) 19–39.

[25] S. Guetersloh, C. Zeitlin, L. Heilbronn, J. Miller, T. Komiyama, A. Fukumura, Y. Iwata, T. Murakami, M. Bhattacharya, Polyethylene as a radiation shielding standard in simulated cosmic-ray environments, Nucl. Instrum. Methods Phys. Res. Sect. B Beam Interact. Mater. Atoms 252 (2) (2006) 319–332, https://doi.org/10.1016/j.nimb.2006.08.019.

[26] A. Villa, L. Barbieri, M. Gondola, A.R. Leon-Garzon, R. Malgesini, An implicit three-dimensional fractional step method for the simulation of the corona phenomenon, Appl. Math. Comput. 311 (2017) 85–99.

[27] A. Villa, L. Barbieri, M. Gondola, A.R. Leon-Garzon, R. Malgesini, Simulation of the AC corona phenomenon with experimental validation, J. Phys. D Appl. Phys. 50 (2017) 435201.

[28] A. Villa, L. Barbieri, M. Gondola, R. Malgesini, An symptotic preserving scheme fo the streamer simulation, J. Comput. Phys. 242 (1) (2013) 86–102.

[29] L. Chen, T. D. Huan, R. Ramprasad, Electronic structure of polyethylene: role of chemical, morphological and interfacial complexity, Sci. Rep. 7 (1). doi:10.1038/s41598-017-06357-y.

[30] C.F. Gallo, W.L. Lama, Classical electrostatic and description of the work and function and ionization energy and of insulators, IEEE Transactions on industry applications IA- 12 (1) (1976) 7–11.

[31] D. Cubero, G. Marcelli, N. Quirke, Electronic states of excess electrons in polyethylene. Annual Report Conference on Electrical Insulation and Dielectric Phenomena, IEEE, 2002.

[32] G. Teyssedre, C. Laurent, Charge transport modeling in insulating polymers: from molecular to macroscopic scale, IEEE Trans. Dielectr. Electr. Insul. 12 (5) (2005) 857–875.

[33] A. Huzayyin, S. Boggs, Density functional analysis of chemical impurities in dielectric polyethylene, IEEE Trans. Dielectr. Electr. Insul. 17 (3).

[34] A. Huzayyin, S. Boggs, R. Ramprasad, Quantum mechanical studies of carbonyl impurities in dielectric polyethylene, IEEE Trans. Dielectr. Electr. Insul. 17 (3).

[35] A. Huzayyin, S. Boggs, R. Ramprasad, Quantum mechanical study of charge injection at the interface of polyethylene and platinum, IEEE (2012) 800–803.

[36] M. Unge, C. Törnkvist, T. Christen, Space charges and deep tra ps in polyethylene – ab initio simulations of chemic al impurities and defects, in: IEEE International Conference on Solid Di Electrics, Bologna, Italy, June 30 – July 4, IEEE, 2013, 2013, pp. 935–939.

[37] L. Chen, H.D. Tran, C. Wang, R. Ramprasad, Unraveling the luminescence signatures of chemical defects in polyethylene, J. Chem. Phys. 143 (12) (2015) 124907, https://doi.org/10.1063/1.4931986.

[38] L. Barbieri, A. Villa, R. Malgesini, A step forward in the characterization of the partial discharge phenomenon and the degradation of insulating materials through nonlinear analysis of time series, IEEE Electr. Insul. Mag. 28 (4).

[39] M. D. Noskov, A. S. Malinovski, M. Sack, A. J. Schwab, Numerical investigation of insulation conductivity effect on electrical treeing, in: Electrical Insulation and Dielectric Phenomena, 1999 Annual Report Conference on, Vol. vol. 2, 2016, pp. 597–600.

[40] L. Testa, S. Serra, G. C. Montanari, Advanced modeling of electron avalanche process in polymeric dielectric voids: simulations and experimental validation, J. Appl. Phys..

[41] N. Hozumi, H. Nagae, Y. Muramoto, M. Nagao, X. HengKyun, Time-lag measurement of void discharges and numerical simulation for clarification of the factor for partial discharge pattern, Inst. Electr. Eng. Japan (2001).

[42] G. Callender, T. Tanmaneeprasert, P.L. Lewin, Simulating partial discharge activity in a cylindrical void using a model of plasma dynamics, J. Phys. Appl. Phys. 52 (5) (2019), 055206.

[43] G. Callender, I.O. Golosnoy, P. Rapisarda, P.L. Lewin, Critical analysis of partial discharge dynamics in air filled spherical voids, J. Phys. Appl. Phys. 51 (2018) 125601.

[44] P. Morshuis, A. Cavallini, G.C. Montanari, F. Puletti, A. Contin, The behavior of physical and stochastic parameters from partial discharges in spherical voids, Proceedings of the 6th International Conference on. Properties and Applications of Dielectric Materials, 2000, 2000.

[45] C. Pan, K. Wu, Y. Du, J. Tang, X. Tao, Y. Luo, Simulation of cavity PD sequences at DC voltage by considering surface charge decay, J. Phys. Appl. Phys..

[46] J. Orloff, Handbook of Charged Particle Optics, second ed., 2008. CRC Press.

[47] A. Villa, L. Barbieri, R. Malgesini, A.R. Leon-Garzon, Ignition of discharges in macroscopic isolated voids and first electron availability, J. Appl. Phys. 125 (4) (2019), 043302, https://doi.org/10.1063/1.5052313.

[48] L.D. Landau, E.M. Lifshitz, Quantum Mechanics: Non-relativistic Theory, third ed., vol. III, 1981. Course of Theoretical Physics.

[49] N.W. Ashcroft, N.D. Mermin, Solid State Physics, Holt, Rinehart and Winston, Cornell University, New York, 1976.

[50] J. Kitchin, Modeling Materials Using Density Functional Theory, 2012.

[51] L.A. Dissado, J.C. Fothergill, Electrical Degradation and Breakdown in Polymers, P. Peregrinus, London, 1992, p. 2.

[52] M.C. Righi, S. Scandolo, S. Serra, S. Iarlori, E. Tosatti, G. Santoro, Surface states and negative electron affinity in polyethylene, Phys. Rev. Lett. 87 (2001), 076802.

[53] M. Loudon, J. Parise, Organic Chemistry, sixth ed., 2016. Freeman, W. H. & Company.

[54] J.D. Hepworth, D.R. Waring, M.J. Waring, Aromatic Chemistry, 2002. Tutorial Chemistry Texts.

[55] P. Giannozzi, S.B.N. Bonini, M. Calandra, R. Car, C. Cavazzoni, D. Ceresoli, G. L. Chiarotti, M. Cococcioni, I. Dabo, A.D. Corso, S. de Gironcoli, S. Fabris, G. Fratesi, R. Gebauer, U. Gerstmann, C. Gougoussis, A. Kokalj, M. Lazzeri, L. Martin-Samos, N. Marzari, F. Mauri, R. Mazzarello, S. Paolini, A. Pasquarello, L. Paulatto, C. Sbraccia, S. Scandolo, G. Sclauzero, A.P. Seitsonen, A. Smogunov, P. Umari, R.M. Wentzcovitch, Quantum ESPRESSO: a modular and open-source software project for quantum simulations of materials, J. Phys. Condens. Matter 21 (2009) 395502.

[56] H.L. Skriver, N.M. Rosengaard, Surface energy and work function of elemental metals, Phys. Rev. B 46 (11) (1992) 7157–7168.

[57] J. Wang, S.Q. Wang, Surface energy and work function of fcc and bcc crystals: density functional study, Surf. Sci. 630 (2014) 216–224.

[58] S.D. Waele, K. Lejaeghere, M. Sluydts, S. Cottenier, Error estimates for densityfunctional theory predictions of surface energy and work function, Phys. Rev. B 94 (2016) 1–13.

[59] D.P. Ji, Q. Zhu, S.Q. Wang, Detailed first-principles studies on surface energy and work function of hexagonal metals, Surf. Sci. 651 (2016) 137–146.

[60] R. Tran, X.-G. Li, J.H. Montoya, D. Winston, K.A. Persson, S.P. Ong, Anisotropic work function of elemental crystals, Surf. Sci. 687 (2019) 48–55, https://doi.org/10.1016/j.susc.2019.05.002.

[61] J.P. Perdew, K. Burke, M. Ernzerhof, Generalized gradient approximation made simple, Phys. Rev. Lett. 77 (1996) 3865–3868.

[62] E. Földes, A. Tóth, E. Kálmán, E. Fekete, Ágnes Tomasovszky-Bobák, Surface changes of corona-discharge-treated polyethylene films, J. Appl. Polym. Sci. 76 (2000) 1529–1541.
[63] R. Morent, N.D. Geyter, C. Leys, L. Gengembre, E. Payen, Comparison between XPS- and FTIR-analysis of plasma-treated polypropylene film surfaces, Surf. Interface Anal. 40 (2008) 597–600.
[64] A.R. Leon-Garzon, G. Dotelli, M. Tommasini, C.L. Bianchi, C. Pirola, A. Villa, A. Lucotti, B. Sacchi, L. Barbieri, Experimental characterization of polymer surfaces subject to corona discharges in controlled atmospheres, Polymers 11 (10) (2019) 1646, https://doi.org/10.3390/polym11101646.
[65] M. Meunier, N. Quirke, A. Aslanides, Molecular modeling of electron traps in polymer insulators: chemical defects and impurities, J. Chem. Phys. 115 (6) (2001) 2876–2881, https://doi.org/10.1063/1.1385160.